International Research Journal of Engineering and Technology (IRJET) e-ISSN: 2395-0056
Volume: 11 Issue: 10 | Oct 2024 www.irjet.net p-ISSN: 2395-0072

Unsteady stagnation point flow of a nanofluid and analysis of binary solutions

Dr. Mariam ALmahdi Mohammed Mulla

Department of Mathematics University of Hafr AL-Batin (UHB) Hafr AL-Batin, KSA

Abstract - *This paper is concerned with unstable fixed-point dual-flow solutions of a nanofluid above a disk moving under the influence of oscillating currents. Standard equations are in two dimensions using appropriate transformations. Choosing appropriate transformations, the partial differential equations (PDEs) representing the heat transfer problem are transformed into ordinary differential equations (ODEs). The basic equations have been solved Using "bvp4c function numerically in MATLAB". The present results are validated with available comparison and a very close accuracy was obtained. A comparison was presented between the solutions we arrived at with the numerical solutions, and this indicates Excellent convergence. To solve in the upper part for all values of nanofluid* α_1, α_2 *circular parameter* Ψ_a*, and attraction Parameter* γ*. However, a change in the bottom solution is observed at some moderate values and in addition, the radial velocity increases due to the nanofluid while the velocity decreases at others. However, the temperature rises due to nanofluids. The results also indicate Until the circular parameter increases its speed in both directions and the temperature decreases. It increases and then decreases with respect to the tangential component of the velocity, but the temperature increases monotonically.*

Key Words: *Unrestricted, Flow axisymmetric flow fluid kinematics, partial differential equations, engineering quantities.*

1.INTRODUCTION

The flow caused by the circular disc has a lot to do with it engineering and industrial applications for example in wastewater treatment, computer storage treatment devices, aerospace technology, stator system, solar thermal manufacturing and geothermal mineral extraction process, The Newtonian fluid was above a steadily rotating disk [1, 2]. Due to the huge impact Magnetic field on flux [3] examined Flow through the circular disc port. Instead, [4] Study multiple solutions for a pure liquid to flow over a rotating disc subject to time Impairing the free, unrestricted flow. you will be the importance of rotating discs in moving turbines [5, 6] by studying the magnetic flux on a rotating disc.[7, 8] The effect of force, ionic slip, and ohmic heating on a steady flow over a rotating disk.[9] developed ideal solutions for magnets and constant and viscous fluid flow the study was carried out taking into account temperature and mass transfer along with thermophysical properties and their variation [10, 11]. In thin liquid bodies on a rotating disk through combined effects. Non-uniform magnetic field, non-linear beam, in many mathematics and engineering applications are significant heat Still enhanced to improve heat [12, 13] A mixture of pure liquids and extremely small nanoparticles is called nanofluids. Nanofluids provide a good heat conduction rate Regular fluids.[14, 15] Flow and heat transfer from the flow of nanofluids across a rotating disc with sliding velocity and magnetic field [16] The phenomenon of conduction and Heat transfer through the study of flow analysis caused by microorganisms and Nanoparticles pass through flexible surfaces with irregular magnetic fields [17] investigated the thermal conductivity and the effect of viscosity on the magnetic rheology induced by Nanofluid from flexible vertical tube. It can be controlled using a pressure gradient via the obviosity parameter. Nanofluids can be produced by dispersing two distinct systems of nanoparticles in Medium of normal liquids. Challenges and applications On nanofluids in Studies [18, 19]. Challenges and applications of nano fluidics in studies [20, 21]. The effect on the flow of electrical forces aided through vessels induced by second-order nanofluids was studied [22, 23]. Flow and heat transfer characteristics were performed [24, 25]. Flow processes for transporting liquids and nanoparticles at high temperature, focusing on flexible ribbons, liquefaction efficiency, supersonic extrusion, etc., are all examples of engineering and technological procedures that need to be studied in extended flow[26, 27]. An examination the implementation of stability can determine the degree to which it can tolerate unsteady flow parameters[28]. It turns out that there are two solutions in a larger space with a higher parameter value. Investigation of nanofluid flow.

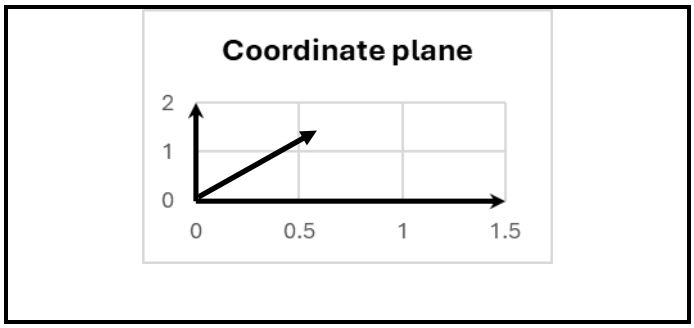

Figure. 1. The axis of flow in systems.

Viscous flow across the rotating body is an emblematic phenomenon in many production processes, especially in

systems Involving turntables. Applications of rotating disc-induced flux can be handled, for example, in a rotating stator system, power generators, machinery in turbines, wastewater treatment, oil and natural gas extraction process, geothermal energy extraction[29], storage devices (computers), and chemical reaction chambers. The thermal effect plays a prominent role in many applications in production and technology [30]. For example, solar cells in front of air currents, the temperature of devices maintained by fans, and the cooling coefficients of nuclear reactors in the case of stopping and cycling when there is a difference in densities in the vertical and horizontal direction of deep nanobodies [31]. Furthermore, the interaction effects of nanofluids are examined which includes the thermal mode and a suitable kinetic parameter and the equation is converted from PDEs to ODEs by using the appropriate transformation. Finally, the influence of different parameters on shows temperature, speed and concentration[32, 33].

2. Mathematical background, model and problem formulation

Unsteady two-dimensional incompressible flow of nanofluids on a stagnation point across a moving surface continuous over time, which depends on the expected external flow. Let us consider the outlines of the present model with flow on a rotating disk as shown in Figure 1. The system can be described in cylindrical coordinates (r_a, θ_a, z_a) and the nanoflow is taken to be the axisymmetric flow to be the given flow configuration Axial model and coordinate system with schematically unstable water-based $Ag - TiO_2$ nanofluid. We consider an unsteady, two-dimensional, incompressible flow that transfers heat and mass and moves in a near-infinite vertical manner the plate is at the stagnation point under the influence of thermal radiation currents and binary interaction. Speed variables (H^*, Q^*) It is considered in binary space coordinates (x, y) at the time indicated by the parameter γ. The external fluid is related to the size of the strain rate $S(\gamma) > 0$ effects on the surface in the y axis[32]. We find the appropriate equation for the nanofluid with energy and transport under the above assumption is:

$$\frac{\partial H^*}{\partial x} + \frac{\partial Q^*}{\partial y} = 0 \tag{1}$$

$$\frac{\partial H^*}{\partial \gamma} + H^*\frac{\partial H^*}{\partial x} + Q^*\frac{\partial Q^*}{\partial y} + \frac{1}{\alpha}\frac{\partial \alpha^*}{\partial x} = Q\left(\frac{\partial^2 H^*}{\partial x^2} + \frac{\partial^2 H^*}{\partial y^2}\right) \tag{2}$$

$$\frac{\partial S^*}{\partial \gamma} + H^*\frac{\partial S^*}{\partial x} + Q^*\frac{\partial S^*}{\partial y} = \alpha\left(\frac{\partial^2 S^*}{\partial x^2} + \frac{\partial^2 S^*}{\partial y^2}\right) + s\left(k_\beta\left(\frac{\partial S^*}{\partial x}\frac{\partial R^*}{\partial x} + \frac{\partial S^*}{\partial y}\frac{\partial R^*}{\partial y}\right) + \frac{k_s}{S_\infty}\left(\left(\frac{\partial S^*}{\partial x}\right)^2 + \left(\frac{\partial S^*}{\partial y}\right)^2\right)^2\right) \tag{4}$$

$$\frac{\partial R^*}{\partial \gamma} + H^*\frac{\partial R^*}{\partial x} + Q^*\frac{\partial R^*}{\partial y} = k_\beta\left(\frac{\partial^2 R^*}{\partial y^2}\right) + \frac{k_s}{S_\infty}\left(\frac{\partial^2 S^*}{\partial y^2}\right) - R(S - S_\infty) \tag{5}$$

In addition, the angular velocity of the disc is and the rotation of the disc is about one of its coordinate axes s = 0, where S_0 is the angular velocity corresponding to the steady state and $t\beta$ is the time. The disk is not connected [31]. The $Ag - TiO_2$ water HNF flow is viscous, incompressible and unstable with the effects of flow fluid lightness and buoyancy coefficient, Current and standing point flow. The disk is located and approaches with a variable speed in the positive $z - axis$ direction, where hf, γ, r and s represent the viscosity coefficient The basic fluid kinematics, time, inviscid velocity, and characteristic constraints have dimension $(1/s\beta)$, where $\gamma s\beta < 1$, respectively. For similar solutions, the magnetic field current of time acts in the $z - axis$ direction, where β_0 is its strength. In addition, the electric field as well as the induced magnetic field are neglected. The HNF flows near the stagnation point with a non-rheological velocity that depends on time and temperature T_∞ The changing temperature of the disk surface is denoted by $T_w = T_\infty + T_0, s\beta$. And $Ag - TiO_2$ are in thermal equilibrium with water. The basic equations that follow the above-mentioned hypotheses are specified as follows [32, 33]:

$$\frac{\partial^2 H_b}{\partial r_b^2} + \frac{H_b}{r_b} + \frac{\partial H_b}{\partial z_b} = 0 \tag{6}$$

$$\frac{\partial^2 w}{\partial x^2} + \frac{\partial w}{\partial x} + w = 0 \tag{7}$$

$$\frac{\partial^2 w}{\partial x^2} = -\frac{\partial w}{\partial x} - w \tag{8}$$

Second-order linear Partial differential equation

$$\frac{d}{dx}\left(e^x w'(x)\right) + e^x w(x) = 0 \tag{9}$$

$$w''(x) + w'(x) + w(x) = 0 \tag{10}$$

$$w(x) = c_1 e^{-x/2}\sin\left(\frac{\sqrt{3}x}{2}\right) + c_2 e^{-x/2}\cos\left(\frac{\sqrt{3}x}{2}\right)$$

$$\frac{\partial w_b}{\partial x_b} + u_b\frac{\partial w_b}{\partial r_b} - \frac{w_b^2}{r_b} + w_b\frac{\partial w_b}{\partial z_b} = -\frac{1}{\gamma_{hnf}}\frac{\partial \gamma}{\partial r_b} + \frac{\mu_{hnf}}{\gamma_{hnf}}\left(\frac{\partial^2 w_b}{\partial r_b^2} + \frac{1}{r_b}\frac{\partial w_b}{\partial r_b} - \frac{w_b}{r^2{}_b} + \frac{\partial^2 w_b}{\partial z_b^2}\right) - \frac{\omega_{inf}\beta^2}{\gamma_{hnf}(1+m^2)}(w_b - mv_b) + f\frac{(\gamma\beta)_{hnf}}{\gamma_{hnf}}(T_b - T_\infty) \tag{11}$$

$$\frac{\partial w_b}{\partial r_b}+u_b\frac{\partial w_b}{\partial r_b}+w_b\frac{w_b^2}{r_b}=-\frac{1}{\gamma_{hnf}}\frac{\partial \gamma}{\partial z_b}+\frac{\mu_{inf}}{\gamma_{hnf}}\left(\frac{\partial^2 w_b}{\partial r_b^2}+\frac{1}{r_b}\frac{\partial w_b}{\partial r_b}+\frac{\partial^2 w_b}{\partial z_b^2}\right) \quad (12)$$

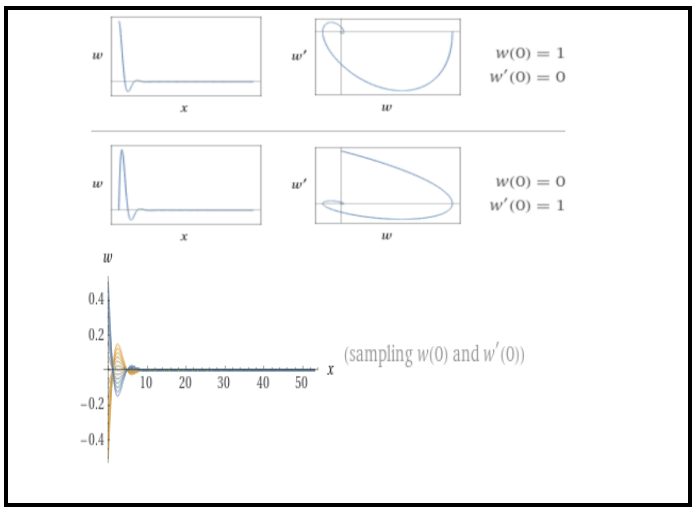

Figure. 2. The flow equation is a linear second-order partial differential equation

where (w_b, v_b, γ_b) are the velocity components along (r_b, θ_b, z_b), g is the acceleration due to gravity, γ is HNF pressure, T_b is HNF temperature, γ_{inf} is HNF density, β_{inf} is HNF thermal expansion, ω_{inf} is HNF electrical conductivity, μ_{inf} is HNF dynamic viscosity,. The boundary conditions associated with the flow are [30, 31]:

$$L(w', w, x)=\frac{1}{2}\left(e^x(w')^2-w^2e^x\right) \quad (13)$$

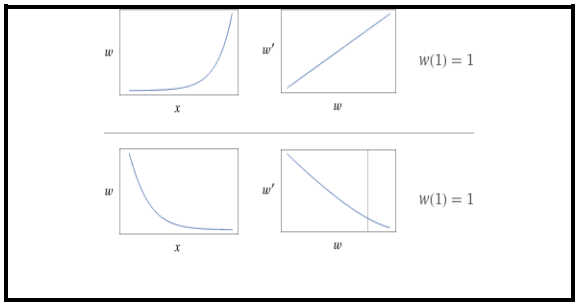

Figure.3. First order nonlinear ordinary differential equations of flow

$$f_r=\frac{4\omega^*}{3k^*}\frac{\partial T^*}{\partial y} \quad (14)$$

k^* is the constant of mean absorption, with ω^* indicating the Stephen-Boltzmann incessant. We assume that there isn't much of a difference in temperature inside the flow [3, 7]. A Taylor series expansion of the equation of (T - $T\infty$) yields the expression T_6, excluding higher-order terms.

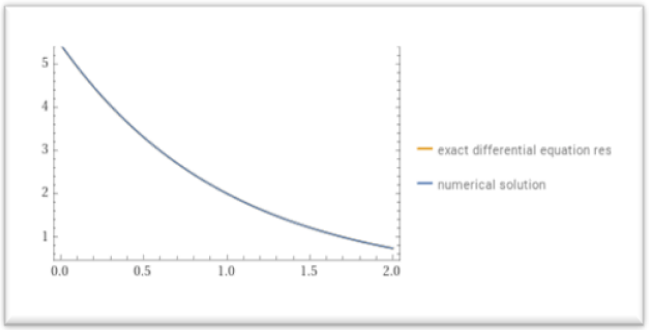

Figure4. For stretching and shrinking flow.

There are boundary conditions that are[11, 14], Boundary conditions considering that the disk is moving in its own plane with speed w^*v which is t times Therefore the free flow velocity produces vx and t is given by

$$v_\omega^*=\gamma v_b^* t^*=t_\omega^* u^*=0, \qquad c^*=c_\omega^* \text{ at } y=0$$

$$v^*=v_b^* t^*=t_\infty^* c^*=c_\infty^* \text{ at } y=\infty$$

The equations and additional terms will be rewritten in different dimensional forms, and non-unidimensional quantities will be used the next one:

$$\bar{x}=\frac{x}{l}, \qquad \bar{y}=\frac{y}{l}, \qquad (\bar{v})^*=\frac{v^* l}{v}, \qquad \bar{v}_p^*=\frac{v_b^*}{u}, \bar{u}^*=\frac{u^* l}{u}$$

$$\bar{t}=\frac{ut}{l^2}, \bar{\gamma}^*=\frac{\gamma^* l^2}{\beta u^2}, \qquad \bar{\Phi}=\frac{\Phi}{u}, \qquad \bar{\delta}_1=\frac{\delta_1}{l}$$

Nanofluids show multiple practical importance in many industries and applications due to the performance and high thermal coefficient from ordinary heat transfer fluid to high heat transfer [10, 17]. Although the instability property can be of unwanted damage, however, no study has touched on the detection of critical issues such as Hybrid nanofluid boundary layer separation and nanofluid flow on a rotating disk. And the intent of the aim of the study is to reveal the features of flow and heat transfer using partial differential equations with demarcation of the boundaries of a layer of unsteady nanofluid flow over a rotating disk in existence of status. Use numerical solutions to basic equations with characteristics of flow that unfolds in a coupled context for solutions. Here we assume the axis of symmetry of the flow in the corresponding cylindrical coordinates $(r; h; z)$ and the change that occurs with respect to h disappears. As the above condition, for the constitutive equations the equations are set as follows[5, 9, 19]:

$$\frac{\partial u}{\partial r}+\frac{\partial v}{\partial z}+\frac{u}{r}=0 \quad (15)$$

$$\gamma_{hnf}\left(\frac{\partial u}{\partial t}+u\frac{\partial u}{\partial r}-\frac{v^2}{r}+w\frac{\partial u}{\partial z}\right) = -\frac{\partial \gamma}{\partial r}+\mu_{hnf}\left(\frac{\partial^2 u}{\partial r^2}+\frac{\partial}{\partial r}\left(\frac{u}{r}\right)+\frac{\partial u^2}{\partial z^2}\right) - \frac{\omega_{hnf}\beta^2}{(1+m^2)}(u-mv) \quad (16)$$

$$\gamma_{hnf}\left(\frac{\partial v}{\partial t}+u\frac{\partial v}{\partial r}+\frac{vu}{r}+w\frac{\partial u}{\partial z}\right)=\mu_{hnf}\left(\frac{\partial^2 v}{\partial r^2}+\frac{\partial}{\partial r}\left(\frac{v}{r}\right)+\frac{\partial^2 v}{\partial z^2}\right)-\frac{\omega_{hnf}\beta^2}{(1+m^2)}(v-mu) \quad (17)$$

$$\gamma_{hnf}\left(\frac{\partial w}{\partial t}+u\frac{\partial w}{\partial r}+w\frac{\partial u}{\partial z}\right)=-\frac{\partial \mu}{\partial z}+\mu_{hnf}\left(\frac{\partial^2 w}{\partial r^2}+\frac{1}{r}\left(\frac{\partial w}{\partial r}\right)+\frac{\partial^2 w}{\partial z^2}\right) \quad (18)$$

Where (u, v, w) are the velocity components along (r, θ, z), f is the acceleration due gravity, μ is HNF temperature, μ_{hnf} is HNFdensity, $\gamma_{hnf}$is HNF thermal expansion ω_{hnf} is HNF electrical conductivity where $\eth w, \partial v, \partial u$ denotes the velocity components in following the respective directions $\partial z, \partial r, \partial t$ is connected to nanofluid pressure, T temperature the nanofluid, ω_{hnf} is the nanofluid density, γ_{hnf} is the viscosity of nanofluids, and m denotes Hall current XC and SC on the frequency and time of electron collision are, respectively, specific heat of nanofluids[12, 21, 25].

$$w_b = 0, v_b = r_b\Phi, u_D = \frac{dH_b}{dt_b} = \frac{\gamma}{2}\sqrt{\frac{v_f}{c(1-\gamma t_b)}}, \quad T_b = T_u = T_\infty + \frac{T_0 r_b}{(1-\gamma t_b)^2}, \quad z_b = H_b(t_0)$$

$$w_b = w_\infty = \frac{cr_b}{(1-\gamma t_b)}, \quad v_b = 0, T_b \to T_\infty, \quad z_b \to \infty$$

Here, stagnation flow strength indicates $b > 0$. Moreover, an external potential flow point difference manipulated fluid flow inside the boundary layer and it denotes the time function t. Substitute in (13) into the governing equations (1)-(12) along with the boundary conditions in (15) and using above similarity variables, in (16), the following equations will be obtained.

3. Stability Analysis

The results display the presence of dual solutions for the tested parameter. Due to the importance of identifying the physically realizable solution, a stability analysis is performed. Following in [1, 27, 30], A dimensionless variable, t, is introduced, which is related to the initial value problem. Dimensionless variables can be represented in equation (18):

$$w = \left(\frac{u}{2lv_f(1-ct)}\right)^{1/2} e^{x/2l}\, y, \Phi = \left(\frac{2lv_f u}{1-ct}\right)^{1/2} e^{x/2l} f(w,r), \quad \theta(w,t) = \frac{T-T_\infty}{T_b-T_\infty},$$

$$r = \frac{ut}{2(1-ct)} e^{x/l}. \quad (20)$$

Equation (20) to get that:

$$\frac{1}{(1-\gamma)^{25}\left(1-\gamma+\gamma\left(\frac{h_{hnf}}{h_f}\right)\right)}\frac{\partial^3 f}{\partial w^3}+f\frac{\partial^2 f}{\partial w^2}-2\left(\frac{\partial f}{\partial w}\right)^2+2-\beta\left(2\frac{\partial f}{\partial w}+w\frac{\partial^2 f}{\partial w^2}-2\right)-\left(2r\frac{\partial f}{\partial w}+2\beta r+1\right)\frac{\partial^2 f}{\partial w \partial r} = 0 \quad (21)$$

$$\frac{1}{h_r}\frac{k_{nf}}{\left(1-\Phi+\Phi\left(\frac{(hc)_s}{(hc)_f}\right)\right)}\frac{\partial^2 f}{\partial w^2}+f\frac{\partial f}{\partial w}-\theta\frac{\partial f}{\partial w}-\beta\left(2\theta+w\frac{\partial \theta}{\partial w}\right) -(1+2\beta r+2r)\frac{\partial \theta}{\partial r}=0 \quad (22)$$

With the following boundary conditions:

$$f(0,r)=\xi, \quad \frac{\partial f}{\partial w}(0,r)=\eta+\omega\frac{\partial^2 f}{\partial w^2}(0,r), \quad \theta(0,r)=1$$

$$\frac{d^2}{dw^2}(f(w)) = f''(w),$$

$$f''(0)+f^{(3)}(0)w+\frac{1}{2}f^{(4)}(0)w^2+\frac{1}{6}f^{(5)}(0)w^3+\frac{1}{24}f^{(6)}(0)w^4+\omega(w^5) \quad (19)$$

Taylor series

$$\frac{\partial f}{\partial w}(w,r)\to 1, \theta(w,r)\to 0, as\ w\to\infty \quad (23)$$

The stable solutions $f(w) = f_0(w)$ and $\theta(w) = \theta_0(w)$ Which satisfy the boundary value problem equations (22), (23) are tested through [30,31]:

$$f(w,r) = f_0(w) + e^{-\gamma r}H(w,r), \quad \theta(w,r) = \theta_0(w) + e^{-\gamma r}G(w,r)$$

where γ is an unknown eigenvalue parameter, $H(w,r)$ and $G(w,r)$ are small corresponding to $f_0(w)$ and $\theta_0(w)$, respectively. The linear problem can be obtained by replacing equation (24) into (23) and (22), as below:

$$\frac{1}{(1-\gamma)^{2.5}\left(1-\gamma+\gamma\left(\frac{h_s}{h_f}\right)\right)}\frac{\partial^3 H}{\partial w^3}+f_0\frac{\partial^2 H}{\partial w^2}-H\left(\frac{\partial f_0}{\partial w}\right)^2-4f_0\frac{\partial H}{\partial w}-\beta\frac{\partial^2 H}{\partial w^2}-2\beta\frac{\partial H}{\partial w}-2\beta\frac{\partial^2 f}{\partial w\partial r}+2\beta r\frac{\partial H}{\partial w}\frac{\partial^2 H}{\partial w\partial r}$$

$$+\gamma\frac{\partial H}{\partial w}-2r\frac{\partial^2 H}{\partial w\partial r}+2r\gamma\frac{\partial H}{\partial w}=0 \qquad (25)$$

$$\frac{1}{h_r}\frac{k_{nf}}{\left(1-\Phi+\Phi\left(\frac{(hc)_s}{(hc)_f}\right)\right)}\frac{\partial^2 G}{\partial w^2}+\beta w\frac{\partial G}{\partial w}-2\beta r\frac{\partial G}{\partial r}-2\beta r\gamma G-\frac{\partial G}{\partial r}+\gamma G-2\beta G-2rf_0'\frac{\partial G}{\partial r}+2\gamma rf_0'G-\theta_0\frac{\partial H}{\partial w}$$

$$-f_0'G+\theta_0'H+f_0'\frac{\partial G}{\partial w}=0 \qquad (26)$$

subject to boundary conditions that:

$$H(0,r)=0,\frac{\partial H(0,r)}{\partial w}+\omega\frac{\partial^2 H(0,r)}{\partial w^2}=0,\ \frac{\partial H(w,r)}{\partial w}\to 0, G(w,r)\to 0\ as\ w\to\infty \qquad (27)$$

We find stability of constant flow $f_0(w)$ and $\theta_0(w)$ It can be tested by $r=0$, for which $H(w)=H_0(w)$ and $G(w)=G_0(w)$ are obtained, indicating initial improvement or contraction as in equation (25). Hence, the linear problem (26) and (27) can be written as follows:

$$\frac{1}{(1-\gamma)^{2.5}\left(1-\gamma+\gamma\left(\frac{h_s}{h_f}\right)\right)}\frac{\partial^3 H_0}{\partial w^3}+f_0\frac{\partial^2 H_0}{\partial w^2}-H_0\left(\frac{\partial f_0}{\partial w}\right)^2-4f_0'\frac{\partial H_0}{\partial w}-\beta w\frac{\partial^2 H_0}{\partial w^2}-(\gamma-2\beta)H_0'$$

$$=0 \qquad (28)$$

$$\frac{1}{h_r}\frac{k_{nf}}{k_f\left(1-\Phi+\Phi\left(\frac{(hc)_s}{(hc)_f}\right)\right)}\frac{\partial^2 G_0}{\partial w^2}+\beta w\frac{\partial G_0}{\partial w}-2\beta rG_0-\theta_0\frac{\partial H_0}{\partial w}-f_0'G_0+\theta_0'H_0+f_0\frac{\partial G_0}{\partial w}+\gamma G_0$$

$$=0 \qquad (29)$$

along with boundary conditions

$$H_0(0)=0,\frac{\partial H_0(0)}{\partial w}+\omega\frac{\partial^2 H_0(0)}{\partial w^2}=0,\ \frac{\partial H_0(w)}{\partial w}\to 0, G_0(w)\to 0\ \ as\ \ w\to\infty \qquad (30)$$

The possible range of the smallest eigenvalue can be found by simplifying the boundary condition $H_0(w)$ or $G_0(w)$ of the proposed issue [16, 20]. In this study, this was determined $\frac{\partial H_0(w)}{\partial w}\to 0$ It should be simplified, and the new boundary condition will be replaced by $H_0(0)=0$

$$\frac{1}{G_b}h(w)-2H^2+\frac{r^2}{8}+2\frac{G_a}{G_b}H'+rH-\frac{r^2}{4}+rGH=C_b \qquad (31)$$

where C_b is the integration constant and its value is evaluated. The value of constant C_b is obtained as zero. Therefore, the non-dimensional form of pressure distribution takes the following form:

$$h(w)=G_b\left(2H^2(w)-2\frac{G_b}{G_b}H'(w)-(1+w)rH(w)+\frac{r^2}{8}\right), \qquad (32)$$

4. The gradients or engineering quantities

The current subsection demonstrates the engineering quantities of interest which are mainly useable in engineering to design equipment at the nanoscale and describe the behavior of the fluid flow through the solution domain. These quantities are mathematically framed as follows:

$$C_{H_r}=\frac{t_{w_2}}{h_f v_\infty^2}, C_{G_r}=\frac{t_{w_2}}{h_f v_\infty^2}\quad Nv_\varphi=\frac{\varphi g_w}{k_f(T_w-T_\infty)},$$

$$r_{w_1}=\mu_{Hnf}\left(\frac{\partial v}{\partial z}\right)_{z=H(t)},\quad r_{w_1}=\mu_{Hnf}\left(\frac{\partial u}{\partial z}\right)_{z=H(t)}, g_w=-k_{Hnf}\left(\frac{\partial T}{\partial z}\right)_{z=H(t)} \qquad (33)$$

where r_{w_1} and r_{w_1} correspond to the shear stresses at the wall surface of the spinning disk and g_w is the respective heat flux at the wall surface of the non-conducting disk. Now substituting (32) into (33), we get the following reduced shear stress, reduced frictional torque, and reduced local Nusselt number. The skin friction or shear stress at the surface of the spinning disk along the radial direction: The frictional torque at the surface of the spinning disk along the azimuthal direction:

$$\sqrt{Re_r}C_{G_r}=\mu_\beta G'(0) \qquad (34)$$ The heat transfer rate at the surface of the spinning disk:

$$Re_r^{-1/2}Nv_r=K_\beta\theta'(0),\quad Re_r=\frac{v_\infty r}{u_f} \qquad (35)$$

Where there is a number $Re_r^{-1/2}Nv_r$. It is called the local dyno number

5. Numerical Methodology

This section demonstrates the dimensionless forms of the linear Partial differential equations along with the appropriate boundary conditions (6), which are difficult to solve analytically. Hence, these equations (15) to (24) are tackled numerically using a built-in function in MATLAB software [3, 9, 33], which is based on finite difference scheme to find their approximate two different solution branches. This method is working in the first order of PDEs.

Here, to continue the process, we need to change our dimensionless equations from higher-order into first order by letting the new variable as follows: The dual solutions of the Partial differential equations (12) to (18), along with the boundary conditions (6), the bvp4c program was used in MATLAB. The proposed formula and its algorithm, based on iteration, are applied to solve the system of equations. Then combining the formula and the polynomial gives w_1-continuous. There are unseen values for the heat transfer coefficient $g_w(0)$ It is obtained by specifying some initial guess values for the parameters tested, and satisfying the field boundary conditions asymptotically. The process of searching for it is repeated until no other solutions can be obtained outside a certain point, which is the point that represents the solution r, or get to another field if the solution point is difficult to obtain, or the solution does not already exist. Points close to the critical values of The first and second solutions are tested using stability analysis to obtain the smallest eigenvalues g_w, To obtain stability of solutions. The smallest eigenvalues can be obtained by solving the linear problem (26), (28) Using the software for both upper and lower solutions. Positive eigenvalues represent a stable solution, while negative eigenvalues represent an unstable solution. (29) With the corresponding initial conditions in Equation (30), the proposals require initial initialization, initial solution points, and differences in the speed of achieving the accuracy goals. 10^6. In addition, the problem is solved numerically for the two different solutions, and two different new guesses are required to obtain distinct results. The result of the upper part can be obtained easily due to the clear estimation, while the estimation required for the lower part is complex. Therefore, choosing the estimate for the lower part requires more effort to obtain solutions that achieve the boundary convergence to be asymptotic.

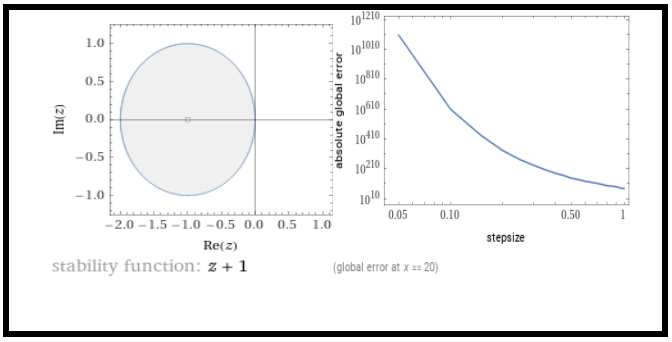

Figure 5. Agree on the surface of the turntable wall and g_w.

6. Discussion

Nanoparticle volume fraction j, velocity slip parameter θ, unsteadiness parameter β stretching/shrinking parameter ω suction/injection parameter s, Types of nanoparticles are studied. As suggested by the water flow model it has few $(Re = 3.2)$ Chosen as the base fluid, the size of the nanoparticles ranges between 0 and 0.2, Nanoparticles do not appear in the basic liquid $j = 0$. A table of thermophysical The properties of water, copper and alumina are studied in Table 1, where the value for each substance is taken from [32, 33]. The work has been validated. [22, 29]We find that the problem is the same $(\beta = 0)$ over a permeable surface $(r = 0)$ with no-slip condition $G_0(w) \to 0 \ as \ w \to \infty$ was considered, as shown in Table 2, We observed a clear agreement. from. (30) indicates excellence in relation ω. Then let:

$$\beta = \frac{S}{S^2}$$

$$\frac{\partial^{(4)}H}{\partial w^4} + \omega\frac{\partial^{(3)}H}{\partial w^{(3)}} - \beta\frac{\partial H}{\partial w}\frac{\partial^{(2)}H}{\partial w^{(2)}} - \frac{s}{s^2}\left(\frac{1}{2}\frac{\partial^{(3)}H}{\partial w^{(3)}} + \frac{3}{2}\frac{\partial^{(2)}H}{\partial w^{(2)}}\right) = 0, \quad (36)$$

Let us consider $\beta \neq 0$, necessary condition for comparison of the current study and integrating above equation as follows

$$S(t) = \frac{1}{\beta(-t + r)}$$

Here r is the steady reference value of time t such that 1, $s(0)\ \beta(-t + r) = 0$ If $\beta = 0$, in (37) produces $s(t)$ such as unvarying 1 and also non-dimensional elements of velocity is mentioned are deduced for stable stagnation-point flow to an inflexible stationary plate highlighted [12, 13]while $a = 1$. Consequently, the dimensionless parameter β calculates the instability power of this current problem and unstable boundary layer flow detaches from stable flow.

$$\frac{\partial^{(4)}H}{\partial w^4} + \omega H\frac{\partial^{(3)}H}{\partial w^{(3)}} - \beta\left(\frac{\partial H}{\partial w} + \frac{1}{2}\frac{\partial^{(2)}H}{\partial w^{(2)}}\right) - \omega\left(\frac{\partial H}{\partial w}\right)^2 = c, \quad (38)$$

where $c = -(\omega + \beta)$ by using the boundary condition and applying in above one

$$\frac{\partial^{(3)}H}{\partial w^{(3)}} - \beta\left(H\frac{\partial^{(2)}H}{\partial w^{(2)}}\right) + \beta - \beta\left(\frac{\partial H}{\partial w}\right)^2 - \beta\left(\frac{1}{2}\frac{\partial^2 H}{\partial w^2} - 1 + \frac{\partial H}{\partial w}\right)^2 = 0, \quad (39)$$

Consider the analytical solution for $\beta = 2\omega$ through employing a function $F(\varphi) = H(\varphi) - \varphi$ transformation such that:

$$H(\varphi) = \varphi + \frac{1 - \lambda}{\sqrt{3\beta + \lambda}}\left(e^{-\sqrt{3\beta+\lambda}\varphi} - 1\right), \quad if \ \sqrt{3\beta} = \sqrt{\lambda} > 0. \quad (40)$$

For more details refer this article [10, 11]. The non-dimensional pressure $Q(Z,\varphi,t)$ distribution is attained by:

$$Q(Z,\varphi,t) = -\left(\frac{(\beta+\alpha)\omega}{2\alpha^2}Z^2 + \frac{\beta}{\alpha(r-t)}\left(\frac{\partial H}{\partial w} + \frac{\beta}{2}H^2 - \frac{\alpha}{2}\varphi H\right)\right) + Q_0(t) \quad (40)$$

where $Q\ (t)$ is called stagnation pressure. The stream function Ω is defined as

$$\Omega = \beta\frac{Z}{\sqrt{\alpha(r-t)}}H(\varphi), \quad \varphi = \frac{X}{\sqrt{\alpha(r-t)}} \quad (41)$$

The engineering interest of in heat and mass transfer flow, local skin friction, f_c local Nusselt number M_u and local Sherwood

number *h S* are defined by:

$$C_f = \frac{2}{H_e(Y,t)^2}\left(\frac{\partial H}{\partial X}\right)_{X=0} = \frac{21}{\beta Y}\sqrt{\alpha(r-t)}\frac{\partial^2 H}{\partial t^2}(0) \quad (42)$$

$$M_w = \frac{Y}{T_\omega - T_\infty}\left(\frac{\partial H}{\partial X}\right)_{X=0} = \frac{Y}{\sqrt{\alpha(r-t)}}\frac{\partial\theta}{\partial t}(0), \quad (43)$$

$$S_h = \frac{Y}{C_\omega - C_\infty}\left(\frac{\partial H}{\partial X}\right)_{X=0} = \frac{Y}{\sqrt{\alpha(r-t)}}\frac{\partial\varphi}{\partial t}(0), \quad (44)$$

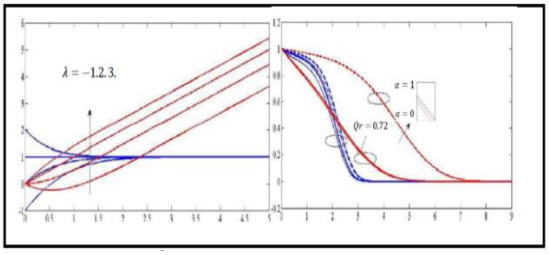

Figure 6. Difference of $\theta(\varphi)$ for dual fixed values of $Qr = 0.72$ and 7 when $\alpha = 0$ and $\lambda = -1,2,3.$ .Difference of $H(\varphi)$ and $\frac{\partial H}{\partial t}(\varphi)$ for various values λ with attached flow solution at (a) $\alpha = 1$ and $\alpha = 0$. Figure 6. Difference of $\theta(\varphi)$ for dual fixed values of $Qr = 0.72$ and 7 when $\alpha = 0$ and

$\lambda = -1,2,3.$ and $\lambda = 1.2,-1,0,0,1.0,1,2.$

and $\lambda = -1,0,1,2.$

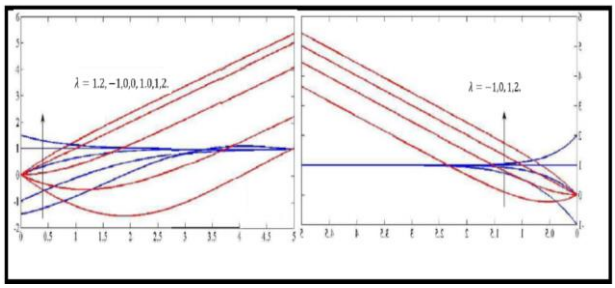

Figure 7. Difference of $H(\varphi)$ and $\frac{\partial H}{\partial t}(\varphi)$ for various values λ with attached flow solution at (a) $\alpha = 1$ and (b) $\alpha = 0.$

6. Discussion

Nanoparticle volume fraction j, velocity slip parameter θ, unsteadiness parameter β stretching/shrinking parameter ω suction/injection parameter s, Types of nanoparticles are studied. As suggested by the water flow model it has few $(Re = 3.2)$ Chosen as the base fluid, the size of the nanoparticles ranges between 0 and 0.2, Nanoparticles do not appear in the basic liquid $j = 0$. A table of thermophysical The properties of water, copper and alumina are studied in Table 1, where the value for each substance is taken from [32, 33]. The work has been validated. [22, 29]We find that the problem is the same $(\beta = 0)$ over a permeable surface $(r = 0)$ with no-slip condition $G_0(w) \to 0\ as\ w \to \infty$ was considered, as shown in Table 2, We observed a clear agreement. from. (30) indicates excellence in relation ω. Then let:

$$\beta = \frac{S}{S^2}$$

$$\frac{\partial^{(4)}H}{\partial w^4} + \omega\frac{\partial^{(3)}H}{\partial w^{(3)}} - \beta\frac{\partial H}{\partial w}\frac{\partial^{(2)}H}{\partial w^{(2)}} - \frac{s}{s^2}\left(\frac{1}{2}\frac{\partial^{(3)}H}{\partial w^{(3)}} + \frac{3}{2}\frac{\partial^{(2)}H}{\partial w^{(2)}}\right) = 0, \quad (36)$$

Let us consider $\beta \neq 0$, necessary condition for comparison of the current study and integrating above equation as follows

$$S(t) = \frac{1}{\beta(-t+r)} \quad (37)$$

Here r is the steady reference value of time t such that 1, $s(0)\ \beta(-t+r) = 0$ If $\beta = 0$, in (37) produces $s(t)$ such as unvarying 1 and also non-dimensional elements of velocity is mentioned are deduced for stable stagnation-point flow to an inflexible stationary plate highlighted [12, 13]while $a = 1$. Consequently, the dimensionless parameter β

calculates the instability power of this current problem and unstable boundary layer flow detaches from stable flow.

$$\frac{\partial^{(4)}H}{\partial w^4}+\omega H\frac{\partial^{(3)}H}{\partial w^{(3)}}-\beta\left(\frac{\partial H}{\partial w}+\frac{1}{2}\frac{\partial^{(2)}H}{\partial w^{(2)}}\right)-\omega\left(\frac{\partial H}{\partial w}\right)^2=c, \tag{38}$$

where $c = -(\omega+\beta)$ by using the boundary condition and applying in above one

$$\frac{\partial^{(3)}H}{\partial w^{(3)}}-\beta\left(H\frac{\partial^{(2)}H}{\partial w^{(2)}}\right)+\beta-\beta\left(\frac{\partial H}{\partial w}\right)^2-\beta\left(\frac{1}{2}\frac{\partial^2 H}{\partial w^2}-1+\frac{\partial H}{\partial w}\right)^2=0, \tag{39}$$

Consider the analytical solution for $\beta = 2\omega$ through employing a function $F(\varphi) = H(\varphi) - \varphi$ transformation such that:

$$H(\varphi)=\varphi+\frac{1-\lambda}{\sqrt{3\beta+\lambda}}\left(e^{-\sqrt{3\beta+\lambda\varphi}-1}\right),\quad if\ \sqrt{3\beta}=\sqrt{\lambda}>0. \tag{40}$$

For more details refer this article [10, 11]. The non-dimensional pressure $Q(Z,\varphi,t)$ distribution is attained by:

$$Q(Z,\varphi,t)=-\left(\frac{(\beta+\alpha)\omega}{2\alpha^2}Z^2+\frac{\beta}{\alpha(r-t)}\left(\frac{\partial H}{\partial w}+\frac{\beta}{2}H^2-\frac{\alpha}{2}\varphi H\right)\right)+Q_0(t) \tag{40}$$

where $Q(t)$ is called stagnation pressure. The stream function Ω is defined as

$$\Omega=\beta\frac{Z}{\sqrt{\alpha(r-t)}}H(\varphi),\quad \varphi=\frac{X}{\sqrt{\alpha(r-t)}} \tag{41}$$

The engineering interest of in heat and mass transfer flow, local skin friction, f_c local Nusselt number M_u and local Sherwood

number *h S* are defined by:

$$C_f=\frac{2}{H_e(Y,t)^2}\left(\frac{\partial H}{\partial X}\right)_{X=0}=\frac{21}{\beta Y}\sqrt{\alpha(r-t)}\frac{\partial^2 H}{\partial t^2}(0) \tag{42}$$

$$M_w=\frac{Y}{T_\omega-T_\infty}\left(\frac{\partial H}{\partial X}\right)_{X=0}=\frac{Y}{\sqrt{\alpha(r-t)}}\frac{\partial\theta}{\partial t}(0), \tag{43}$$

$$S_h=\frac{Y}{C_\omega-C_\infty}\left(\frac{\partial H}{\partial X}\right)_{X=0}=\frac{Y}{\sqrt{\alpha(r-t)}}\frac{\partial\varphi}{\partial t}(0), \tag{44}$$

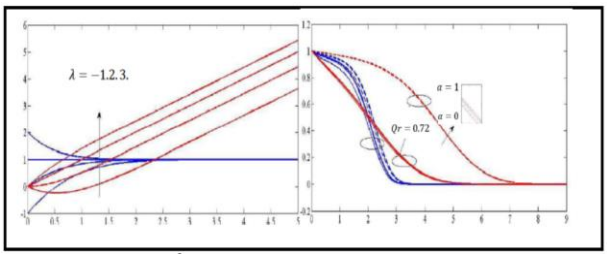

Figure 6. Difference of $\theta(\varphi)$ for dual fixed values of $Qr = 0.72$ and 7 when $\alpha = 0$ and $\lambda = -1,2,3.$.

Difference of $H(\varphi)$ and $\frac{\partial H}{\partial t}(\varphi)$ for various values λ with attached flow solution at (a) $\alpha = 1$ and $\alpha = 0$. Figure 6. Difference of $\theta(\varphi)$ for dual fixed values of $Qr = 0.72$ and 7 when $\alpha = 0$ and

$\lambda = -1,2,3.$ and $\lambda = 1.2,-1,0,0,1.0,1,2.$ and $\lambda = -1,0,1,2.$

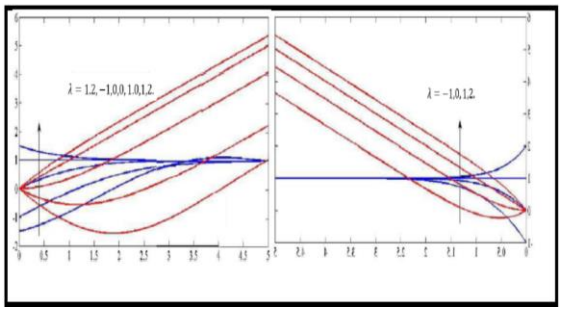

Figure 7. Difference of $H(\varphi)$ and $\frac{\partial H}{\partial t}(\varphi)$ for various values λ with attached flow solution at (a) $\alpha = 1$ and (b) $\alpha = 0$.

7. Interpretation of the numerical solution

In our numerical scheme leads us to the following upper and lower solution branches for the dimensionless along with the boundary stipulation (28) which notice that diverse flow patterns may appear in certain spectrums of physical constraints $h\ and\ \Phi$ and nanoparticles volume fraction $^1/_2$ and $^1/_2$. It is important to note that the two different branches' outcomes are mathematically sound and can be well-matched with the engineering, physics, and mechanics of the flow phenomena. The computational outcomes of the friction factor, $\mu_A\frac{\partial^2 H}{\partial w^2}(0)$, frictional torque, $\mu_A\frac{\partial G}{\partial w}(0)$ and Nusselt number, $k_A\frac{\partial\theta}{\partial w}(0)$, of the water $Ag-TiO_2$ HNF are designed against the impingement parameter α_A, for the specified changing values of the

rotation parameter $\Phi_A = (1.0\ and\ 0.2)$. respectively. The similarity solution for the water-based $Ag - TiO_2$ hybrid nanofluid exists for all negative choices of the impingement parameter α_A, for the situation of the upper branch when $\Phi_A = 1.0$. On the other hand, the existence of the similarity solution is completely terminating in the range of $-1.0 < \alpha_A < \infty$, in the phenomenon of the lower branch solution, where a critical or bifurcation value at $\alpha_A = -1.0$.

Table 1. The current of two branches solutions with the result when $\Phi_A = \varphi_1 = \varphi_2 = m = M_A$ [33].

α	Upper Branch solutions	Upper Branch solutions	Current upper solution	Current lower solution
0.0	1.933	–	2.94463	–
−0.2	1.930	–	2.93421	–
−0.5	1.926	11.067	2.90324	12.19863
−0.6	1.923	9.764	2.99543	9.56432
−1.0	1.814	5.654	2.86431	6.67549
−1.5	1.802	5.642	2.87523	5.85643
−2.0	1.708	4.854	2.73245	4.86232
−2.5	1.705	4.764	2.76543	4.75634
−3.0	1.606	3.962	2.62345	3.86427

Table 2 Value of the stress at the surface of the disk along the direction formula several values of the parameters when $m = 0.5,\ \ \alpha_A = -1.0\ \ and\ Qr = 3.2$

k_1, k_2	Φ_A	M_A	$\mu_A \frac{\partial^2 H}{\partial w^2}$	
			Upper Branch	Lower Branch
0.20	1.0	0.5	1.45567730	−1.87732621
0.25	–	–	1.46366420	−1.87843276
0.30	–	–	1.48543723	−1.87808763
0.35	0.0	0.5	1.52566891	−1.92507843
0.25	1.0	–	1.55643216	−0.87865210
–	2.0	0.1	1.58762181	−2.43783297
–		0.3	1.55077443	−1.54678216
–		0.2	1.55988324	−1.54648214

Table 3 Value of the frictional at the surface of the disk along the azimuthal direction for several values of the parameters when $m = 0.5,\ \ \alpha_A = -1.0\ \ and\ Qr = 3.2$

k_1, k_2	Φ_A	M_A	$\mu_A \frac{\partial^2 G}{\partial w^2}$	
			Upper Branch	Lower Branch
0.20	1.0	0.5	−1.65432	−2.06574
0.25	–	–	−1.68742	−1.67843
0.30	–	–	−1.65478	−1.87308
0.35	0.0	0.5	−0.20547	−0.82507
0.25	1.0	–	−1.05633	−1.07835
–	2.0	0.1	−2.08743	−2.46783
–		0.3	−0.45327	−2.54478
–		0.2	−0.43622	−2.94648

8. CONCLUSIONS

The study addresses the unsteady stagnation point flow of nanofluids across a moving flat surface and the time-dependent inviscid outward flow velocity and constant surface temperature. Taking the characteristics of the thermal situation, movement, and chemical reaction parameters into account. The management system was converted into a system of ODEs that uses similarity transformations, and the results are implemented using the RK method. An important finding was highlighted: $\frac{\partial H}{\partial w}(\varphi)$ The horizontal velocity rises are represented with increasing values 0 > 0 and $\frac{\partial H}{\partial w}(\varphi)$ occurring so that they have an inverted position for the boundary layer and the velocity ratio parameter is taken let $t > 1$ for the attached flow solution. It represents a streamline pattern of residual flux associated with a larger $\lambda > 0$, separated from the plate surface for a smaller $\lambda < 0$ and then compared to the stable stagnation fixed point flow $\lambda = 0$. The coil is optimized for energy $\theta(\varphi)$ with increasing thermal mode parameter(Nt) with coupled fluid for attached flow without deflection and flow with deflection. We obtain a concentration distribution to increasing function of the reaction coefficient Cr. The effect of convection with varying temperature on the flow of $Ag - TiO_2$ water on a rotating disk was studied with some effects. The rheology of

$Ag - TiO_2$ water nanostructures were studied for two cases: assisted rheology and counter rheology. The mathematical model is solved via the "bvp4c function

accessible via MATLAB". We obtained important results of this investigation:

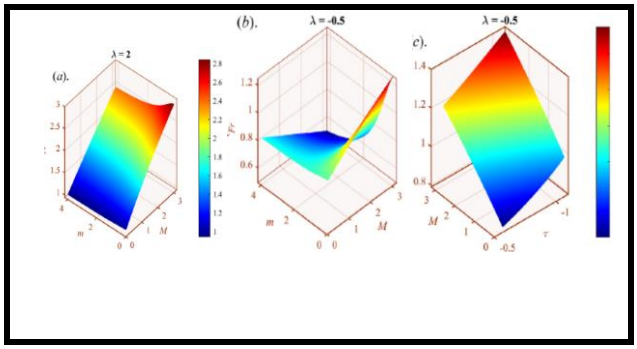

Author Contributions The manuscript was written by the author. The results were discussed with peers and the final version of the manuscript was reviewed.

Acknowledgments The authors wish to acknowledge the reviewers whose comments helped improve this manuscript.

Conflict of Interest The author declared no potential conflicts of interest with respect to the research, authorship, and publication of this article.

REFERENCES

[1] Yang, J., et al., *Deposition of oral bacteria and polystyrene particles to quartz and dental enamel in a parallel plate and stagnation point flow chamber.* Journal of colloid and interface science, 1999. **220**(2): p. 410-418.

[2] Rasool, G. and A. Wakif, *Numerical spectral examination of EMHD mixed convective flow of second-grade nanofluid towards a vertical Riga plate using an advanced version of the revised Buongiorno's nanofluid model.* Journal of Thermal Analysis and Calorimetry, 2021. **143**(3): p. 2379-2393.

[3] Pavithra, G.M. and B.J. Gireesha, *Unsteady flow and heat transfer of a fluid-particle suspension over an exponentially stretching sheet.* Ain Shams Engineering Journal, 2014. **5**(2): p. 613-624.

[4] Rao, J.A., G. Vasumathi, and J. Mounica, *Joule heating and thermal radiation effects on MHD boundary layer flow of a nanofluid over an exponentially stretching sheet in a porous medium.* World Journal of Mechanics, 2015. **5**(09): p. 151-164.

[5] Wong, S.W., A.O. Awang, and A. Ishak, *Stagnation-point flow over an exponentially shrinking/stretching sheet.* Zeitschrift für Naturforschung A, 2011. **66**(12): p. 705-711.

[6] Sahoo, B., R.A. Van Gorder, and H. Andersson, *Steady revolving flow and heat transfer of a non-Newtonian Reiner–Rivlin fluid.* International communications in heat and mass transfer, 2012. **39**(3): p. 336-342.

[7] Attia, H.A., *On the effectiveness of ion slip on steady MHD flow and heat transfer above a rotating disk with Ohmic heating.* 2006.

[8] Akram, S., et al., *Double-diffusivity convection on Powell–Eyring nanofluids in non-uniform inclined channel under the impact of peristaltic propulsion and induced magnetic field.* The European Physical Journal Plus, 2021. **136**(5): p. 494.

[9] Tiwari, R.K. and M.K. Das, *Heat transfer augmentation in a two-sided lid-driven differentially heated square cavity utilizing nanofluids.* International Journal of heat and Mass transfer, 2007. **50**(9-10): p. 2002-2018.

[10] Ebrahimi, A., et al., *Heat transfer and entropy generation in a microchannel with longitudinal vortex generators using nanofluids.* Energy, 2016. **101**: p. 190-201.

[11] Abu-Nada, E. and H.F. Oztop, *Numerical analysis of Al2O3/water nanofluids natural convection in a wavy walled cavity.* Numerical Heat Transfer, Part A: Applications, 2011. **59**(5): p. 403-419.

[12] Kuznetsov, A. and D. Nield, *The Cheng–Minkowycz problem for natural convective boundary layer flow in a porous medium saturated by a nanofluid: a revised model.* International Journal of Heat and Mass Transfer, 2013. **65**: p. 682-685.

[13] Najib, N., et al., *Boundary layer flow and heat transfer of nanofluids over a moving plate with partial slip and thermal convective boundary condition: Stability analysis.* International Journal of Mechanics, 2017. **11**(1): p. 18-24.

[14] Hafidzuddin, E.H., et al., *Stability analysis of unsteady three-dimensional viscous flow over a permeable stretching/shrinking surface.* Journal of Quality Measurement and Analysis, 2015. **11**(1): p. 19-31.

[15] Roşca, A.V. and I. Pop, *Mixed convection stagnation-point flow past a vertical flat plate with a second order slip.* Journal of heat transfer, 2014. **136**(1): p. 012501.

[16] Noor, A., R. Nazar, and K. Jafar, *Stability analysis of stagnation-point flow past a shrinking sheet in a nanofluid.* Journal of Quality Measurement and Analysis, 2014. **10**(2): p. 51-63.

[17] Pour, M.S. and S.G. Nassab, *Numerical investigation of forced laminar convection flow of nanofluids over a backward facing step under bleeding condition.* Journal of Mechanics, 2012. **28**(2): p. N7-N12.

[18] Che Sidik, N.A., N. Yen Cheong, and A. Fazeli, *Computational Analysis of Nanofluids in Vehicle Radiator.* Applied Mechanics and Materials, 2015. **695**: p. 539-543.

[19] Hady, F., et al., *Boundary-layer flow in a porous medium of a nanofluid past a vertical cone.* An Overview of Heat Transfer Phenomena; Kazi, SN, Ed.; IntechOpen: London, UK, 2012: p. 91-104.

[20] Noghrehabadi, A., R. Pourrajab, and M. Ghalambaz, *Effect of partial slip boundary condition on the flow and heat transfer of nanofluids past stretching sheet prescribed constant wall temperature.* International Journal of Thermal Sciences, 2012. **54**: p. 253-261.

[21] Wang, C., *Stagnation flow towards a shrinking sheet.* International Journal of Non-Linear Mechanics, 2008. **43**(5): p. 377-382.

[22] Alqahtani, B., et al., *Heat and mass transfer analysis of MHD stagnation point flow of carbon nanotubes with convective stretching disk and viscous dissipation.* Advances in Mechanical Engineering, 2022. **14**(10): p. 16878132221128390.

[23] Din, A., *The stochastic bifurcation analysis and stochastic delayed optimal control for epidemic model with general incidence function.* Chaos: An Interdisciplinary Journal of Nonlinear Science, 2021. **31**(12).

[24] Takhar, H.S., A.J. Chamkha, and G. Nath, *Flow and mass transfer on a stretching sheet with a magnetic field and chemically reactive species.* International Journal of Engineering Science, 2000. **38**(12): p. 1303-1314.

[25] Glassman, I., *PHYSICS OF FLAMES (U).* 1970.

[26] Afify, A.A., *MHD free convective flow and mass transfer over a stretching sheet with chemical reaction.* Heat and Mass Transfer, 2004. **40**(6): p. 495-500.

[27] Kandasamy, R., K. Periasamy, and K.S. Prabhu, *Effects of chemical reaction, heat and mass transfer along a wedge with heat source and concentration in the presence of suction or injection.* International journal of heat and mass transfer, 2005. **48**(7): p. 1388-1394.

[28] Mahmood, Z., et al., *Unsteady MHD stagnation point flow of ternary hybrid nanofluid over a spinning sphere with Joule heating.* International Journal of Modern Physics B, 2022. **36**(32): p. 2250230.

[29] Mahmood, Z., et al., *Ternary hybrid nanofluid near a stretching/shrinking sheet with heat generation/absorption and velocity slip on unsteady stagnation point flow.* International Journal of Modern Physics B, 2022. **36**(29): p. 2250209.

[30] Mahmood, Z. and U. Khan, *Nanoparticles aggregation effects on unsteady stagnation point flow of hydrogen oxide-based nanofluids.* The European Physical Journal Plus, 2022. **137**(6): p. 750.

[31] Mahmood, Z., et al., *Influence of suction and heat source on MHD stagnation point flow of ternary hybrid nanofluid over convectively heated stretching/shrinking cylinder.* Advances in Mechanical Engineering, 2022. **14**(9): p. 16878132221126278.

[32] Adnan, et al., *Thermal transport investigation and shear drag at solid–liquid interface of modified permeable radiative-SRID subject to Darcy–Forchheimer fluid flow composed by γ-nanomaterial.* Scientific Reports, 2022. **12**(1): p. 3564.

[33] Cheng, J. and S. Dai, *A uniformly valid series solution to the unsteady stagnation-point flow towards an impulsively stretching surface.* Science China Physics, Mechanics and Astronomy, 2010. **53**: p. 521-526.